1521-0103/358/3/441–449$25.00
THE JOURNAL OF PHARMACOLOGY AND EXPERIMENTAL THERAPEUTICS

http://dx.doi.org/10.1124/jpet.116.234591
J Pharmacol Exp Ther 358:441–449, September 2016

Class I Histone Deacetylase Inhibition for the Treatment of Sustained Atrial Fibrillation[S]

Mitsuru Seki,[1] Ryan LaCanna,[1] Jeffery C. Powers,[1] Christine Vrakas,[1] Fang Liu, Remus Berretta, Geena Chacko, John Holten, Pooja Jadiya, Tao Wang, Jeffery S. Arkles, Joshua M. Copper, Steven R. Houser, Jianhe Huang, Vickas V. Patel, and Fabio A. Recchia

Cardiovascular Research Center (M.S., R.L.C., J.C.P., C.V., R.B., G.C., Jo.H., P.J., T.W., S.R.H., Ji.H., V.V.P., F.A.R.), and Section of Clinical Cardiac Electrophysiology (J.S.A., J.M.C., V.V.P.), Lewis Katz School of Medicine, Temple University, Philadelphia, Pennsylvania; Institute of Life Sciences, Scuola Superiore Sant'Anna, Pisa, Italy (F.A.R.); and Children's Hospital of Philadelphia, Philadelphia, Pennsylvania (F.L.)

Received April 23, 2016; accepted June 22, 2016

ABSTRACT

Current therapies are less effective for treating sustained/permanent versus paroxysmal atrial fibrillation (AF). We and others have previously shown that histone deacetylase (HDAC) inhibition reverses structural and electrical atrial remodeling in mice with inducible, paroxysmal-like AF. Here, we hypothesize an important, specific role for class I HDACs in determining structural atrial alterations during sustained AF. The class I HDAC inhibitor *N*-acetyldinaline [4-(acetylamino)-*N*-(2-amino-phenyl) benzamide] (CI-994) was administered for 2 weeks (1 mg/kg/day) to Hopx transgenic mice with atrial remodeling and inducible AF and to dogs with atrial tachypacing-induced sustained AF. Class I HDAC inhibition prevented atrial fibrosis and arrhythmia inducibility in mice. Dogs were divided into three groups: 1) sinus rhythm, 2) sustained AF plus vehicle, and 3) sustained AF plus CI-994. In group 3, the time in AF over 2 weeks was reduced by 30% compared with group 2, along with attenuated atrial fibrosis and intra-atrial adipocyte infiltration. Moreover, group 2 dogs had higher atrial and serum inflammatory cytokines, adipokines, and atrial immune cells and adipocytes compared with groups 1 and 3. On the other hand, groups 2 and 3 displayed similar left atrial size, ventricular function, and mitral regurgitation. Importantly, the same histologic alterations found in dogs with sustained AF and reversed by CI-994 were also present in atrial tissue from transplanted patients with chronic AF. This is the first evidence that, in sustained AF, class I HDAC inhibition can reduce the total time of fibrillation, atrial fibrosis, intra-atrial adipocytes, and immune cell infiltration without significant effects on cardiac function.

Introduction

Atrial fibrillation (AF) is the most common cardiac arrhythmia in clinical practice, afflicting almost 3 million Americans and over 45 million individuals worldwide (Naccarelli et al., 2009; Zoni-Berisso et al., 2014). Most of these patients (75–85%) suffer from either sustained or permanent AF with some form of heart disease and atrial remodeling (Murin et al., 2014), which is defined as any structural or electrical alteration that predisposes the atrium to arrhythmias. Evidence supports the contribution of atrial remodeling and fibrosis to the genesis of AF, and conversely, reduced atrial fibrosis correlates with less AF in both paroxysmal and permanent forms (Li et al., 2001; Liu et al., 2008; Marrouche et al., 2014). This may explain why most patients with permanent AF are less responsive to current antiarrhythmic or catheter-based therapies (Gaita et al., 2008; Cappato et al., 2010), which do not prevent or reduce atrial remodeling.

Inflammation is implicated in the pathogenesis of sustained AF (Guo et al., 2012), whereas anti-inflammatory agents can reduce its onset and recurrence (Abbaszadeh et al., 2012; Yu et al., 2012). Atrial stretch and injury caused by heart failure or by AF itself recruits inflammatory cells that release proinflammatory cytokines, such as interleukin (IL)-1β and tumor necrosis factor (TNF), to the atrium. These cytokines regulate ion channel function (Grandy and Fiset, 2009; Grandy et al., 2010; El Khoury et al., 2014) and the expression of extracellular cellular matrix modulators (Siwik et al., 2000) possibly involved in the mechanisms underlying atrial remodeling. Proinflammatory cytokines also induce the release of profibrotic cytokines, such as transforming growth factor-β1 and platelet-derived growth factor, which recruit and stimulate the differentiation of myofibroblasts and fibroblasts (Friedrichs et al., 2011). Finally, inflammatory cytokines

This work was supported by the National Institutes of Health [Grants R01 HL105734 to V.V.P. and R01 HL108213 to F.A.R.] and unrestricted funds from the Lewis Katz School of Medicine at Temple University.
[1]M.S., R.L., J.C.P., and C.V. contributed equally to this work.
dx.doi.org/10.1124/jpet.116.234591.
[S] This article has supplemental material available at jpet.aspetjournals.org.

ABBREVIATIONS: AF, atrial fibrillation; ANOVA, analysis of variance; CI-994, *N*-acetyldinaline [4-(acetylamino)-*N*-(2-amino-phenyl) benzamide]; HDAC, histone deacetylase; Hopx^{Tg}, transgenic mice overexpressing the transcription factor homeodomain-only protein; IL, interleukin; LV, left ventricle; MR, mitral regurgitation; TNF, tumor necrosis factor.

produced by adipocytes and macrophages in visceral and epicardial adipose deposits (Vieira-Potter, 2014) may further contribute to the genesis of AF (Lin et al., 2012; Venteclef et al., 2015). Of note, only mature immune cells and adipocytes release inflammatory cytokines, and class I histone deacetylases (HDACs) promote the differentiation and maturation of these cell types (Haberland et al., 2010; Yamaguchi et al., 2010; Summers et al., 2013). We previously showed that the pan–histone deacetylase inhibitor trichostatin A reverses established atrial fibrosis and inducible atrial arrhythmias, without affecting cardiac chamber size, function, or hemodynamics in transgenic mice overexpressing the transcription factor homeodomain-only protein ($Hopx^{Tg}$), a model of ventricular hypertrophy (Liu et al., 2008). This was the first report documenting the role played by HDACs in atrial remodeling and arrhythmias in animals with structural heart disease. Subsequently, other groups have confirmed our findings and shown that pan-HDAC (Lkhagva et al., 2014) or HDAC6 (Zhang et al., 2014) inhibition can prevent subacute atrial electrical remodeling and inducible AF. Although these results are encouraging, it is not known yet whether HDAC inhibition can oppose the development of sustained AF, the form with higher clinical impact.

In the present study, we hypothesize an important role for class I HDAC in driving chronic atrial remodeling by promoting proinflammatory cytokine release during sustained AF (see Supplemental Fig. 1). Therefore, the class I HDAC inhibitor *N*-acetyldinaline [4-(acetylamino)-*N*-(2-amino-phenyl) benzamide] (CI-994), a cytostatic anticancer agent (Pauer et al., 2004; Undevia et al., 2004; Monneret, 2005), was first tested in $Hopx^{Tg}$ mice with atrial remodeling and inducible arrhythmias and then in a clinically relevant canine model of sustained AF. Atrial tissue obtained from transplanted patients with AF and terminal heart failure was used for comparison to identify possible analogies between the histologic alterations reversed by HDAC inhibition in the canine model and those found in the human disease.

Materials and Methods

An expanded methods section is available in the Supplemental Material.

All the procedures in animals were approved by the Temple University Committee on Use and Care of Animals and complied with National Institutes of Health guidelines.

Transgenic Mice. $Hopx^{Tg}$, in which the murine *Hopx* cDNA is overexpressed in cardiomyocytes under control of the α-myosin heavy-chain promoter, has been previously described (Liu et al., 2008). Surface ECG and invasive mouse electrophysiology studies of atrial arrhythmia inducibility were performed as previously described (Ismat et al., 2005; Li et al., 2005; Liu et al., 2008, 2015; Yuan et al., 2010) in 16 $Hopx^{Tg}$ mice (aged 14–17 weeks) and 16 age-matched nontransgenic wild-type littermates of both sexes, in equal proportions. CI-994 (1 mg/kg/day) or vehicle (20% dimethylsulfoxide) was administered intraperitoneally for 2 weeks. The high selectivity of CI-994 for class I HDACs has been previously documented (Bradner et al., 2010).

Dog Instrumentation. Fifteen purpose-bred male dogs (22–25 kg) were chronically instrumented as previously described (Mitacchione et al., 2014; Woitek et al., 2015). First, anesthesia was induced using propofol (6 mg/kg i.v.) and maintained with 1.5–2% isoflurane during 40% oxygen/60% air ventilation. A thoracotomy was then performed in the left fifth intercostal space and a catheter was placed in the descending thoracic aorta, a solid-state pressure gauge (P6.5; Konigsberg Instruments, Pasadena, CA) was inserted into the left ventricle (LV) through the apex, and a Doppler flow transducer (Craig Hartley, Houston, TX) was placed around the left circumflex coronary artery. Wires and catheters were run subcutaneously to the intrascapular region. Prior to closing the chest, an implantable loop recorder (Reveal XT; Medtronic Inc., Minneapolis, MN) was placed subcutaneously over the left atrium. The chest was then closed in layers, and the pneumothorax was reduced. Antibiotics were given after surgery, and the dogs were allowed to fully recover for at least 10 days. After recovery, a pacemaker (Consulta CRT-P; Medtronic Inc.) was implanted subcutaneously, and an atrial lead inserted into the right atrium.

Pacing Protocol in Dogs. Three days after the pacemakers were implanted, dogs were assigned to either the sham-pacing ($n = 5$) or the atrial tachypacing group ($n = 10$). Sham-paced animals had pacemakers programmed in the sense-only mode. High-rate pacing was induced using a custom software protocol provided by Medtronic Inc., first at 210 bpm for 3–4 days, then 400 bpm for 3–4 days, and finally at 600 bpm for the following 21–28 days. If AF was detected, the pacemakers would switch modes and not pace. Pacemakers resumed pacing only if AF stopped and sinus rhythm was detected. Persistent AF was defined as episodes lasting $\geq$3 days without reversal to sinus rhythm. Once the animals remained in AF for at least 3 days, the pacemakers in the tachypaced group were reprogrammed to sense-only mode, and the animals were treated with CI-994 (1.0 mg/kg/day, $n = 5$) or vehicle (20% dimethylsulfoxide, $n = 5$) for 14 days through an intravascular catheter. This dose of CI-994, similar to the one used in mice, was chosen based on a previous systematic toxicological study in rats and dogs that found pathologic alterations at $>$2 mg/kg/day (Graziano et al., 1997). Our goal was the maximal possible inhibition of class I HDAC with a subtoxic dose. All of the animals were euthanized at the end of the drug-infusion period. The pacemakers and implantable loop recorders were interrogated weekly.

Electrogram Acquisition and Processing. The persistence of sinus rhythm was verified in sham-paced dogs, and pacemaker memories were checked to detect spontaneous AF episodes. Two recording modalities were obtained daily from all dogs during follow-up using the pacemaker right atrium–lead intracardiac electrogram, and the implantable loop recorder single-lead recording (left atrial far-field signal).

Hemodynamic Measurements in Dogs. During the cardiac pacing protocol, hemodynamic measurements were taken every week from conscious dogs placed on the laboratory table, as previously described (Mitacchione et al., 2014; Woitek et al., 2015). The aortic catheter was attached to a strain-gauge transducer to measure aortic pressure. LV pressure was measured using the solid-state pressure gauge. Blood flow in the left circumflex coronary artery was measured with a pulsed Doppler flow meter (model 100; Triton Technology, San Diego, CA). All signals were digitally stored via an analog-digital interface (Notocord hem evolution; Notocord Croissy-sur-Seine, France) at a sampling rate of 250 Hz. Digitized data were analyzed offline by the Notocord software. The parameters were captured during one respiratory cycle and comprised heart rate; mean aortic pressure; LV end-diastolic, peak systolic, and end-systolic pressure; mean blood flow in the left circumflex coronary artery; and the maximum and minimum of the first derivative of LV pressure.

Serum Cytokine Measurements in Dogs. Serum cytokine and adipokine levels were measured in blood obtained from the aorta and coronary sinus of dogs before atrial-tachypacing, after sustained AF was induced, and after 2 weeks of CI-994 or vehicle infusion using enzyme-linked immunosorbent assay performed by the National Institutes of Health–supported Metabolomics Center at the University of California (Davis, CA). Cardiac-derived cytokine production was calculated as the cytokine concentration in the coronary sinus serum minus that in the aorta, multiplied by the coronary flow rate.

Histology and Immunohistochemistry. Detailed protocols for histology have been previously described (Liu et al., 2008, 2015). The primary antibodies used were rabbit polyclonal anti-CD19 antibody

(R&D Systems, Minneapolis, MN), rabbit polyclonal anti-CD4 antibody (Abcam, Cambridge, UK), rabbit polyclonal anti-CD163 antibody (Santa Cruz Biotechnology, Dallas, TX), rabbit polyclonal anti-CD68 antibody (Abcam), rabbit polyclonal anti–Perilipin-1 (Santa Cruz Biotechnology), rabbit polyclonal anti–Pref-1 antibody (Santa Cruz Biotechnology), rabbit polyclonal anti-TNFα antibody (Santa Cruz Biotechnology), rabbit polyclonal anti–IL-6 antibody (Santa Cruz Biotechnology), rabbit polyclonal antileptin antibody (Santa Cruz Biotechnology), or rabbit polyclonal antiadiponectin antibody (Santa Cruz Biotechnology). Sections were incubated with Alexa488 or Alexa594 rabbit anti-mouse or goat anti-rabbit secondary antibodies (Thermo Fisher Scientific, Waltham, MA) for fluorescent images, or using the secondary antibody for horseradish peroxidase staining (Abcam). Sections were analyzed using a Nikon TE200 (Nikon Instruments Inc., Tokyo, Japan) microscope equipped with a charge-coupled device camera and epifluorescence capabilities or a Zeiss LSM 510 confocal microscope (Zeiss, Oberkochen, Germany). All histologic analyses were performed in a blinded manner.

Statistical Analysis. Differences in means among multiple data sets were analyzed using one- or two-way analysis of variance (ANOVA) with treatment or presence of atrial fibrillation as the independent factors. When ANOVA showed significant differences, pairwise comparisons between means were tested using Tukey post-hoc analysis. When data were not normally distributed, ANOVA on ranks was used with the Kruskal-Wallis test, followed by pairwise comparison using the Dunn test. Data sets with smaller sample sizes ($n \leq 5$) were compared using the Wilcoxon rank sum test. All values are reported as the mean $\pm$ 1 S.E.M. A probability value <0.05 was considered significant.

Results

Class I HDAC Inhibition Reduces Atrial Remodeling, AF Induction, and Markers of B Cells and Adipocytes in Mouse Atria. As shown in Fig. 1, class I HDAC inhibition with CI-994 completely prevented the development of atrial fibrosis and atrial arrhythmia inducibility in Hopx^{Tg} mice, similar to the effects we previously observed using pan-HDAC inhibition in this model (Liu et al., 2008). Arrhythmia and other cardiac parameters are summarized in Supplemental Table 1. However, similar to the majority of genetic mouse models of arrhythmias (Riley et al., 2012), Hopx^{Tg} mice do not develop the spontaneous or sustained AF that is often associated with atrial remodeling in clinical populations. Therefore, to determine if class I HDAC inhibition reverses atrial remodeling associated with sustained AF, we tested CI-994 in a dog model that more closely mimics the characteristics of the human disease.

Class I HDAC Inhibition Reduces Atrial Remodeling and Sustained AF in Dogs. Dogs with AF developed increased left atrial size and mitral regurgitation (MR) with no significant effect on ventricular ejection fraction, cardiac output, blood pressure, or coronary perfusion compared with control dogs in sinus rhythm (Table 1). However, when we scanned the ECG records at the end of the protocol, we found that dogs in sustained AF infused with CI-994 had experienced phases of sinus rhythm, and over the 2 weeks of infusion, their percentage of time of fibrillation was reduced by 30% compared with dogs receiving only vehicle (Fig. 2, A–C). Dogs in sustained AF receiving CI-994 also had slightly reduced MR but no significant difference in cardiac chamber size or function (Table 1).

Atrial tissue was then analyzed to assess the effects of AF and CI-994 on structural remodeling. First, we performed histologic analysis of trichrome-stained sections of right and left atrial tissue. Fibrosis was increased in both atria of dogs with sustained AF and vehicle infusion compared with those in sinus rhythm. AF dogs infused with CI-994 displayed less atrial fibrosis compared with AF dogs infused with vehicle, but still more than dogs in sinus rhythm (Fig. 2, D–K). In addition, trichrome staining revealed regions with unstained vacuoles consistent with the presence of intramyocardial adipocytes (Fig. 2, D–K), which was confirmed by immunohistochemical

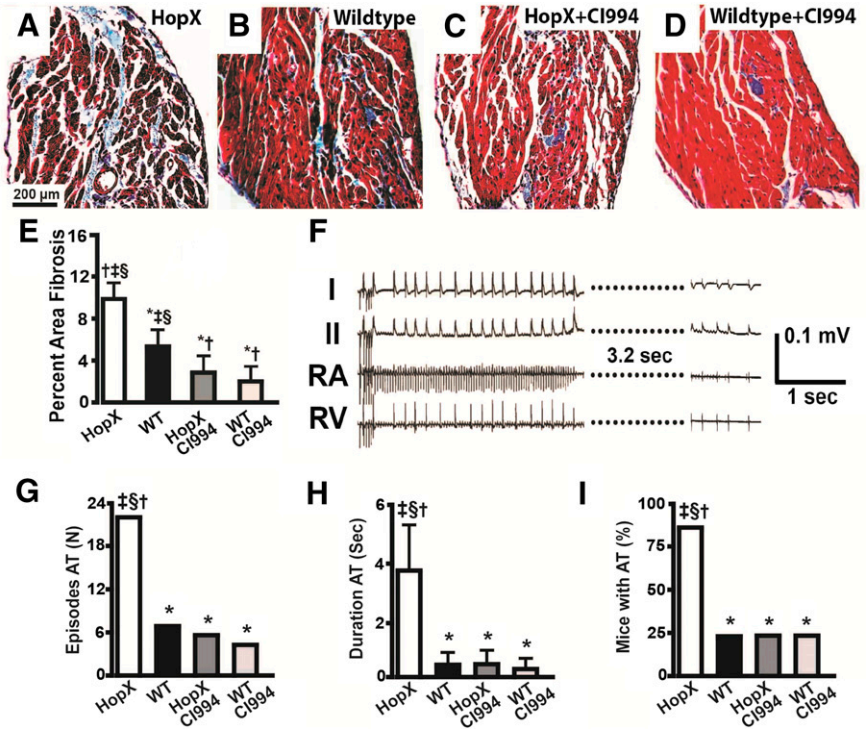

Fig. 1. Inhibiting class I HDACs reduces atrial remodeling and arrhythmias in Hopx transgenic mice. Trichrome-stained images of the left atrium from HopX^{Tg} (A), wild-type (B), HopX^{Tg} mouse treated with CI-994 (C), and wild-type mouse treated with CI-994 (D). (E) Plot showing percentage of atrial fibrosis from at least 26 fields/atrium and four different atria/group. (F) An episode of induced atrial arrhythmia in a Hopx^{Tg} mouse. (G) Number of atrial tachyarrhymia (AT) episodes induced in each group of eight mice. (H) Average duration of induced AT episodes in each group. (I) Percentage of mice with inducible AT in each group of eight mice. $^{*}P < 0.05$ versus Hopx^{Tg}; $^{\dagger}P < 0.05$ versus WT (wild type); $^{\ddagger}P < 0.05$ versus Hopx–CI-994; $^{\S}P < 0.05$ versus WT–CI-994.

TABLE 1
Echo and hemodynamic data from dogs with AF
MR grade based on Doppler flow criteria with 1 = mild, 2 = moderate, 3 = severe, and 4 = torrential.

	Sinus Rhythm Control (n = 5)	Sustained AF + Vehicle Infusion (n = 5)	Sustained AF + CI-994–Treated (n = 5)
LA EDL axis (cm)	2.8 ± 0.30†,‡	3.6 ± 0.55*	3.7 ± 0.49*
LA volume (ml)	18.0 ± 1.3†,‡	30.2 ± 2.5*	33.7 ± 5.3*
LV diastolic size (cm)	4.4 ± 0.32	4.7 ± 0.38	4.8 ± 0.40
MR grade	0.4 ± 0.54†,‡	2.3 ± 0.5*,†	2.8 ± 1.1*,‡
LVEF (%)	62.0 ± 2.8	58.5 ± 1.1	57.4 ± 3.1
Heart rate (bpm)	93.8 ± 18.6†,‡	156.3 ± 36.6*	165.6 ± 18.8*
Coronary flow (ml/min)	60.8 ± 7.5	53.4 ± 5.8	55.2 ± 8.8
dP/dt max. (mm Hg/s)	3209 ± 140†,‡	2149 ± 318*	2083 ± 308*
LV EDP (mm Hg)	5.1 ± 1.3†,‡	9.2 ± 1.5*	10.1 ± 1.8*
LV ESP (mm Hg)	133.1 ± 11.0	119.9 ± 10.9	121 ± 16.5

LA, left atrium; EDL, end-diastolic long; EDP, end-diastolic pressure; ESP, end-systolic pressure.
*$P < 0.05$ versus control; †$P < 0.05$ versus CI-994; ‡$P < 0.05$ versus tachypacing.

staining with antibodies specific for differentiated adipocytes (Perilipin-1) and preadipocytes (Pref-1). Sustained AF caused a significant increase in atrial Perilipin-1- and Pref-1–stained cells compared with atria from dogs in sinus rhythm, or AF dogs treated with CI-994 (Fig. 3). These results suggest that inhibiting class I HDACs reverses atrial remodeling and AF duration in a model with sustained AF, independent of effects on hemodynamics or cardiac function. Furthermore, these findings suggest that class I HDACs in sustained AF contribute to the increased presence of adipocytes. The higher number of Perilipin-1–positive cells in the atrium from dogs in sustained AF, which was attenuated by CI-994, also suggests that class I HDACs may induce dedifferentiation of intra-atrial adipocytes.

To further explore the tissue alterations occurring during sustained AF, we performed immunohistochemical analysis using antibodies against CD19 to quantify B cells, antibodies against CD4 to identify helper T cells, and antibodies against CD163 to mark macrophages. Left atrial sections of dogs with sustained AF displayed more B cells and macrophages compared with those in sinus rhythm, and this alteration was prevented by CI-994 (Fig. 4). However, we detected fewer CD4+ cells in the atrium of dogs with sustained AF compared with those with sinus rhythm.

Class I HDAC Inhibition Reduces Serum and Left Atrial Inflammatory Cytokines in Dogs. Next, we assessed the concentration of inflammatory cytokines and adipokines in the plasma of dogs before atrial tachypacing and after 2 weeks of sustained, postpacing AF without and with CI-994 administration. Blood samples were collected from the aorta and coronary sinus to determine whether cytokines were released by the heart. Cardiac-derived TNFα, IL-6, IL-8, IL-10, and adiponectin increased with sustained AF in the serum and some were almost normalized by class I HDAC inhibition (Table 2). Of note, increased serum levels of these cytokines and adipokines in the serum have been reported in patients with sustained AF as well (Liuba et al., 2008; Shimano et al., 2008; Ozcan et al., 2014). However, serum levels of IL-10 and resistin

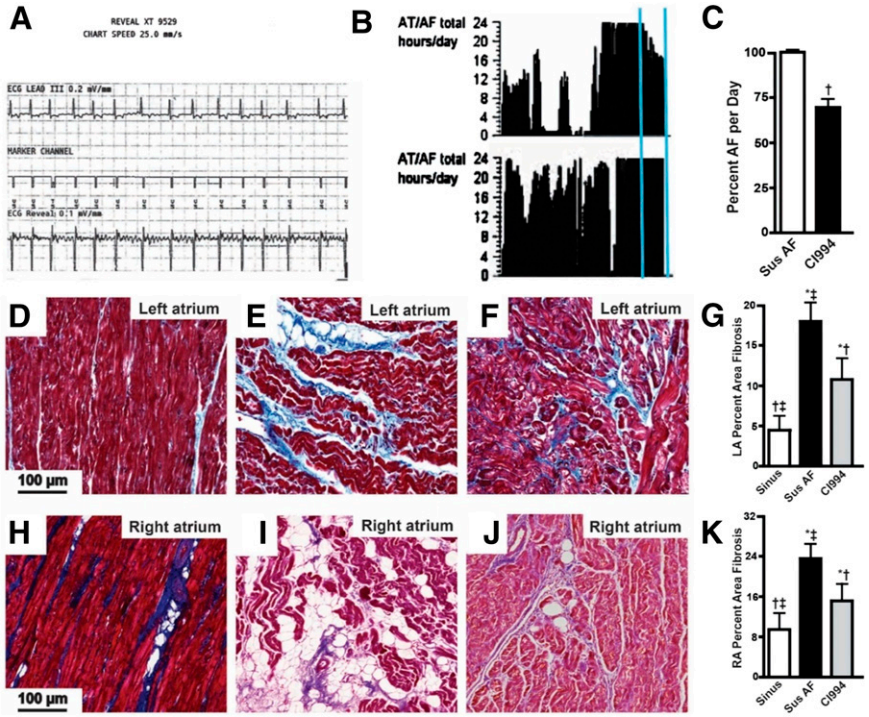

Fig. 2. CI-994 reduces atrial fibrillation and fibrosis in dogs. (A) A typical ECG trace recorded by the Reveal monitor and showing the presence of sustained AF at the end of the atrial pacing period, before vehicle or CI-994 infusions were started. Vertical box = 0.1 mV, horizontal box = 200 ms. (B) Reveal histogram showing hours/day dogs were in AF. Top panel is from a dog treated with CI-994, bottom panel is from a dog given vehicle for the last 2 weeks (vertical lines). (C) Plot of percentage of time dogs were in AF, with and without CI-994 treatment. The CI-994-treated dogs were in AF for ~30% fewer hours/day than the vehicle-treated dogs. Trichrome-stained sections of the posterior left atrium (D–F) and posterior right atrium (H–J) from dogs in sinus rhythm (D and H), dogs in AF plus vehicle for the last 2 weeks (E and I), and dogs in AF treated with CI-994 for the last 2 weeks (F and J). Scale bar in (D) applies to (D–F) and (H–J). (G and K) The percentage of fibrosis averaged from at least 22 images and 5 dogs/group from the left and right atrium, respectively. *$P < 0.05$ versus sinus rhythm (Sinus); †$P < 0.05$ versus sustained (Sus) AF; ‡$P < 0.05$ versus CI-994. AT, atrial tachyarrhymia; LA, left atrium; RA, right atrium.

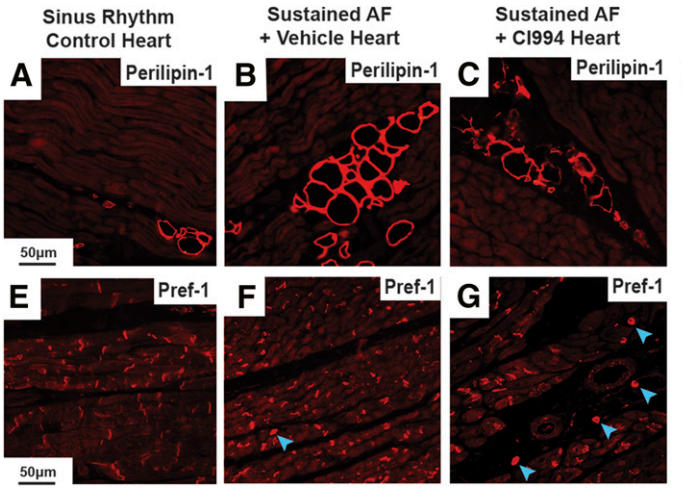

Fig. 3. CI-994 reduces atrial adipocytes in dogs with sustained AF. Immunostaining of canine left atrial sections with antibodies against Perilipin-1 (A–C) and Pref-1 (E–G) from control dogs in sinus rhythm (A and E), dogs with atrial tachypacing-induced sustained AF (B and F), and dogs with sustained AF treated with CI-994 (C and G). Blue arrowheads point out positively stained Pref-1 cells with visible nuclei; there is nonspecific Perf-1 staining against intercalated disks. Scale bar in the left-hand panel applies to that row. (D and H) Comparison of the differences in positive staining for each marker between groups as an average of at least 24 images from five different hearts/group. $^{*}P < 0.05$ versus sinus rhythm (sinus); $^{\dagger}P < 0.05$ versus sustained (Sus) AF; $^{\ddagger}P < 0.05$ versus CI-994.

were not higher during AF. On the other hand, angiotensin II and adiponectin increased in systemic circulation during AF and remained elevated after class I HDAC inhibition, which supports our previous finding that HDAC inhibition may be independent of angiotensin II signaling in atrial remodeling (Liu et al., 2008). The elevated circulating cytokines in AF were consistent with histologic evidence in atrial tissue. The inflammatory cytokines TNFα and IL-6, as well as the adipokines leptin and adiponectin, were more highly expressed in the atrium of dogs in AF compared with those in sinus rhythm, and this increase was attenuated by CI-994 (Supplemental Fig. 2).

Atrial Immune Cells and Intra-atrial Adipocytes in Humans with Chronic AF. The aforementioned results show that class I HDAC inhibition reverses atrial remodeling in the atria of Hopx^{Tg} mice. Moreover, in the dog model of sustained AF, the reversal of atrial fibrosis by CI-994 is associated with reduced B cell infiltration and adipocyte differentiation. But how relevant is the presence of atrial B cell infiltration and adipocyte development in clinical AF? To address this question, we performed histologic analysis of atrial tissue obtained from transplanted patients with AF and end-stage heart failure. First, we analyzed trichrome-stained sections of the right and left atrium from failing human hearts in sinus rhythm and found there was more atrial fibrosis and adipocyte-like vacuoles compared with nonfailing, control, normal hearts in sinus rhythm in both atria (Fig. 5). Moreover, failing hearts with chronic AF had significantly more atrial fibrosis and adipocyte-like vacuoles compared with the atria from failing hearts in sinus rhythm (Fig. 5). Interestingly, based on the documented etiology of heart failure, we found that hearts failing from severe MR displayed the largest amount of fibrosis and intra-atrial adipocytes (Supplemental Fig. 3). Since patients with end-stage heart disease due to severe MR developed the most extensive atrial remodeling, we focused on atrial samples from this group. On these, we performed immunohistochemical analysis with antibodies specific for Perilipin-1 and Pref-1 to determine if the intra-atrial

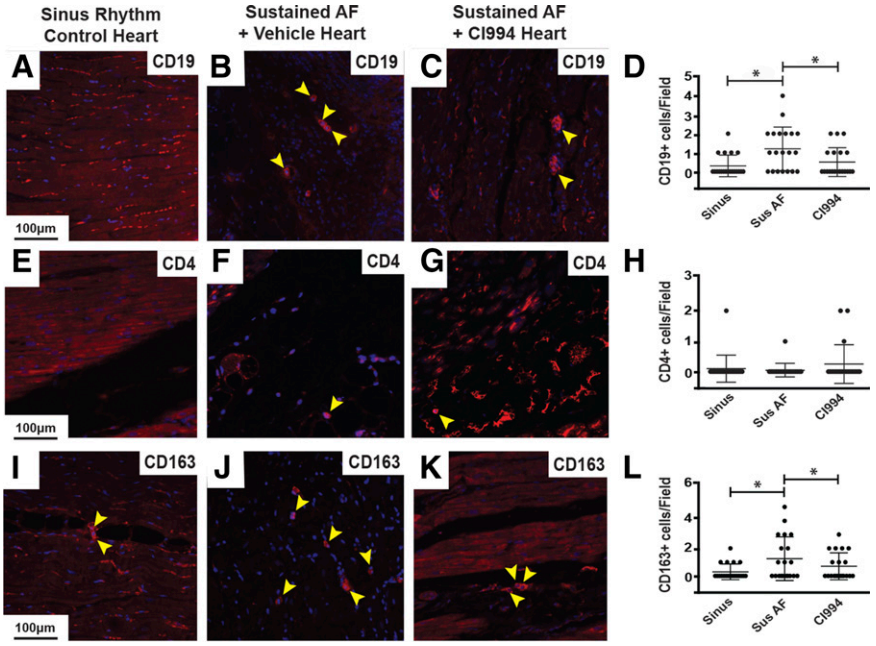

Fig. 4. CI-994 reduces atrial immune cell infiltration in dogs with sustained AF. Immunostaining of canine left atrial sections with antibodies against CD19 to identify B cells (A–C), CD4 to label helper T cells (E–G), and CD163 to mark macrophages (I–K) from control dogs in sinus rhythm (A, E, and I), dogs with atrial tachypacing-induced sustained AF (B, F, and J), and dogs with sustained AF treated with CI-994 (C, G, and K). Blue staining is 4,6-diamidino-2-phenylindol to identify nuclei. Yellow arrowheads point out positively stained cells with stained nuclei. Scale bar in the left-hand panel applies to that row. (D, H, and L) Comparison of the number of CD19+, CD4+, and CD163+ cells per image, respectively. Twenty total images were analyzed from five different hearts/group for each marker. CI-994, sustained atrial fibrillation plus CI-994; Sinus, sinus rhythm; Sus, sustained. $^{*}P < 0.05$.

TABLE 2
Serum cytokine levels in dogs with AF

Cardiac-Derived Production	Sinus Rhythm Control (n = 5)	Sustained AF + Vehicle Infusion (n = 5)	Sustained AF + CI-994–Treated (n = 5)
TNF (pg/h)	3.2 ± 0.9*	64 ± 21†‡	3.5 ± 1.1*
IL-1β (pg/h)	0.1 ± 0.1	0.2 ± 0.1	0.2 ± 0.1
IL-6 (pg/h)	0.5 ± 0.2*,†	52 ± 18†,‡	2.4 ± 1.2*,‡
IL-8 (pg/h)	0.3 ± 0.1*,†	28 ± 10†,‡	1.9 ± 1.0*,‡
IL-10 (pg/h)	0.2 ± 0.2*,†	3.3 ± 0.9‡	2.9 ± 0.7*,‡
Ang-II (ng/h)	0.1 ± 0.1*,†	0.3 ± 0.1†,‡	0.5 ± 0.1*,‡
Resistin (ng/h)	0.1 ± 0.1	0.2 ± 0.1	0.3 ± 0.2
Adipoq. (μg/h)	0.3 ± 0.1*,†	2.1 ± 0.9‡	2.0 ± 1.1‡
Leptin (ng/h)	0.1 ± 0.1	0.3 ± 0.2	0.2 ± 0.1

Adipoq., adiponectin; Ang, angiotensin.
*$P < 0.05$ versus AF; †$P < 0.05$ versus CI-994; ‡$P < 0.05$ versus control.

vacuoles are adipocytes. These studies showed that left atria from patients with end-stage valvular heart disease and chronic AF displayed significantly more Perilipin-1–positive, intra-atrial adipocytes and Pref-1 staining compared with patients with end-stage valvular disease in sinus rhythm (Fig. 6). Importantly, echocardiographic assessment just prior to heart explant showed that ventricular function was not different between patients in sinus rhythm and chronic AF, but patents in AF had left atria that were ~25% larger (Supplemental Table 2).

Next, we used immunohistochemical analysis to assess immune cell infiltration in atria from patients with and without chronic AF using the same antibodies as for the dog tissue analysis. These studies showed more B cells and macrophages infiltrating the atrium during chronic AF compared with sinus rhythm (Fig. 7). However, similar to our findings in the dog model, there were fewer helper T cells in the atrium of patients with chronic AF and heart failure compared with those in sinus rhythm and heart failure (Fig. 7). Finally, the inflammatory cytokines TNFα and IL-6, as well as the adipokines leptin and adiponectin, were more highly expressed in atria from patients with AF and heart failure compared with those in sinus rhythm with either nonfailing or failing hearts (Supplemental Fig. 4).

Taken together, these findings suggest that, in addition to fibrosis, pronounced adipocyte and immune cell infiltration are atrial histologic hallmarks of sustained AF. Moreover, the striking similarities between human and canine histologic alterations support the clinical relevance of our dog model of sustained AF.

Discussion

Our results support an important role for class I HDACs in the pathogenesis of sustained AF. Prompted by the beneficial effects of class I HDAC inhibition on atrial remodeling and inducible AF in a genetic mouse model of ventricular hypertrophy, we subsequently tested this intervention in a more clinically relevant canine model of sustained AF, where it intermittently restored sinus rhythm and reduced fibrosis and other histologic alterations found in clinical AF. The majority of AF patients present with atrial structural remodeling and permanent forms that do not respond well to current antiarrhythmic or ablative therapies. Therefore, the fact that inhibiting class I HDACs can reduce existing atrial remodeling and re-establish phases of sinus rhythm during sustained AF is highly significant and may lead to more effective therapies for patients with permanent AF. Previous studies have shown that HDAC inhibitors oppose electrical and structural remodeling (Liu et al., 2008; Lkhagva et al., 2014; Zhang et al., 2014), but none of them tested these effects in a model of sustained AF.

AF is an adult-onset disease that afflicts increasing numbers of patients (Naccarelli et al., 2009; Zoni-Berisso et al., 2014). The rising incidence of AF is a side effect of improved therapies that improve the survival of individuals with heart failure or prior myocardial infarction. Many of these patients

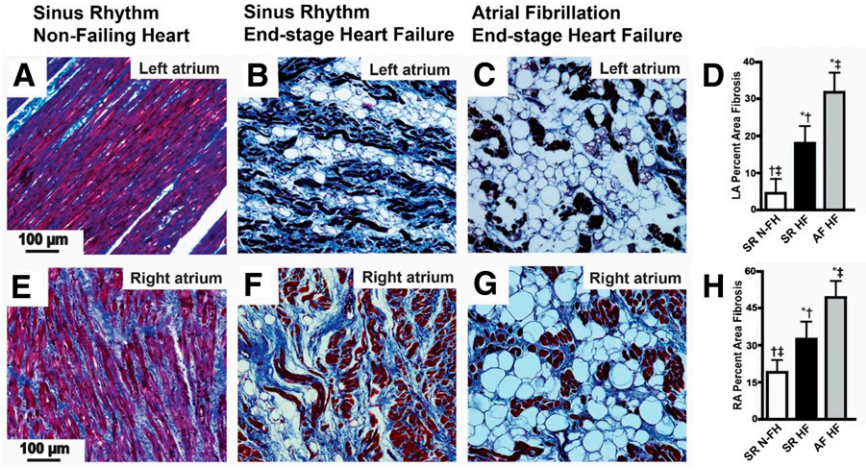

Fig. 5. Heart failure and chronic AF increase atrial fibrosis and adipocytes. Trichrome-stained sections of human left atrium (LA) (A–C) and right atrium (RA) (E–G) from a patient in sinus rhythm without heart failure (A and E), a patient in sinus rhythm with end-stage heart failure (B and F), and a patient with chronic AF and end-stage heart failure (C and G). Scale bar in the left-hand panel applies to all panels in that row. (D and H) Comparison of the percentage of area of atrial fibrosis between these groups in the left and right atrium, respectively, averaged from 20 images or more from three different hearts/group. HF, heart failure; N-FH, nonfailing heart; SR, sinus rhythm. *$P < 0.05$ versus SR N-FH; †$P < 0.05$ versus SR HF; ‡$P < 0.05$ versus AF HF.

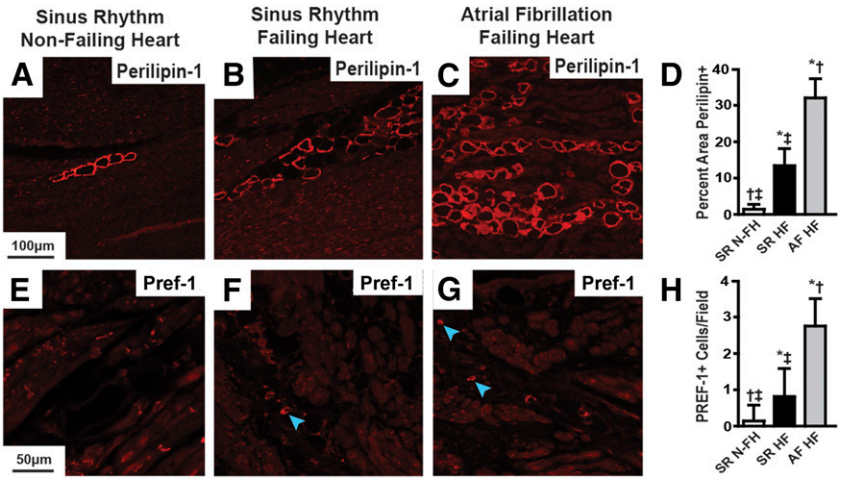

Fig. 6. Heart failure and chronic AF increase atrial adipocytes. Immunostaining of human left atrial sections with antibodies against Perilipin-1 (A–C) and Pref-1 (E–G) from patients in sinus rhythm without heart failure (A and E), patients in sinus rhythm with end-stage heart failure (B and F), and patients with chronic AF and end-stage heart failure (C and G). Blue arrowheads point out positively stained Pref-1 cells with visible nuclei. Scale bar in the left-hand panel applies to that row. (D and H) Comparison of the differences in positive staining for each marker between groups as an average of at least 24 images from three different hearts/group. HF, heart failure; N-FH, nonfailing heart; SR, sinus rhythm. $^{*}P < 0.05$ versus SR N-FH; $^{\dagger}P < 0.05$ versus SR HF; $^{\ddagger}P < 0.05$ versus AF HF.

have ventricular dysfunction that elevates intracardiac pressure on the thinner-walled atrium, which induces chronic inflammation and, in turn, structural remodeling and a predisposition to sustained AF. HDACs, in particular class I HDACs, promote the maturation of adipocytes and inflammatory cells that produce inflammatory cytokines (Haberland et al., 2010; Summers et al., 2013). In our dog model, we could assess not only atrial and circulating levels of TNFα and interleukins but also their cardiac production, which increased during AF and was mostly normalized by CI-994.

Increased Adipocytes with Atrial Remodeling in Sustained AF. In dogs with sustained AF, class I HDAC inhibition prevented the pathologic increase in mature atrial adipocytes. Although the contribution of obesity to AF is well established, and adipocytes have been shown to directly influence atrial myocyte electrophysiology (Lin et al., 2012), our findings suggest that the increase in adipocytes is a significant component of atrial structural remodeling in sustained AF that may lead to the release of inflammatory adipokines within the atrial myocardium. The appearance of intra-atrial adipocytes in the remodeled atrium, confirmed in atrial samples from patients with AF, may be related to the fact that mesenchymal precursors, which give rise to preadipocytes, are also fibroblast precursors and can differentiate into either adipocytes or fibroblasts (Liu et al., 2009). Increased intra-atrial adipocytes can contribute directly to the arrhythmogenic substrate by creating barriers to electrical conduction, as well as releasing inflammatory cytokines and adipokines that influence atrial myocyte electrophysiology and induce fibrosis.

B Cell Infiltration in Atrial Remodeling with Sustained AF. B cell infiltration of the atrium during sustained AF was an unexpected discovery. Although it has been appreciated for some time that lymphocytes infiltrate the atrium during AF, almost all of the evidence implicates T cells in this process (Yamashita et al., 2010). However, newer evidence suggests that B cells may actually drive inflammation by recruiting T cells in some diseases, such as obesity and

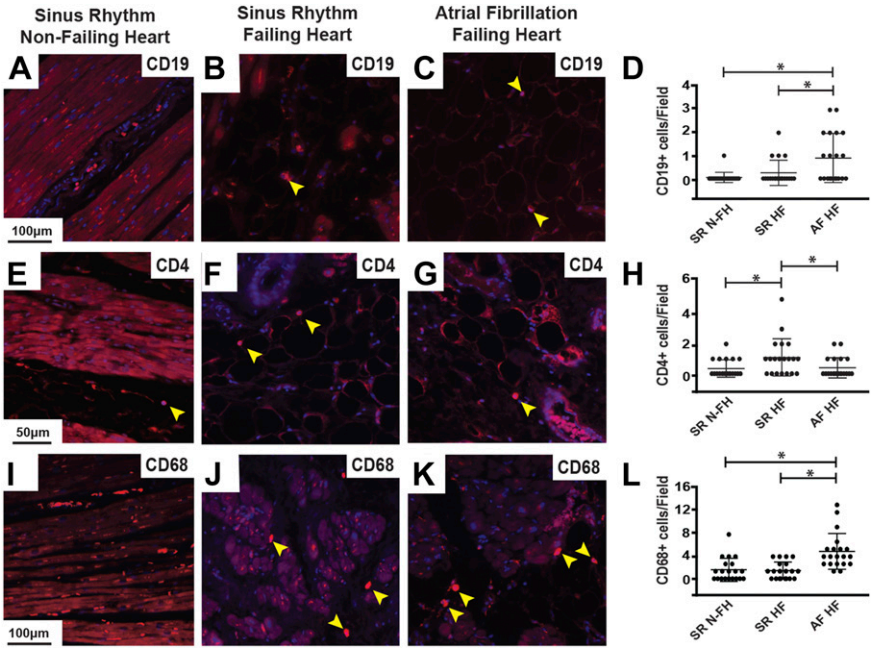

Fig. 7. Heart failure and chronic AF increase atrial immune cell infiltration. Immunostaining of human left atrial sections with antibodies against CD19 to identify B cells (A–C), CD4 to detect helper T cells (E–G), and CD68 to mark macrophages (I–K) from patients in sinus rhythm without heart failure (A, E, and I), patients in sinus rhythm with end-stage heart failure (B, F, and J), and patients with chronic AF and end-stage heart failure (C, G, and K). Yellow arrowheads point out positively stained cells with stained nuclei. Blue staining is 4,6-diamidino-2-phenylindol to identify nuclei. Scale bar in the left-hand panel applies to that row. (D, H, and L) Comparison of the number of CD19+, CD4+, and CD68+ cells per image, respectively. Twenty total images were analyzed from three different hearts/group for each marker. HF, heart failure; N-FH, nonfailing heart; SR, sinus rhythm. $^{*}P < 0.05$.

diabetes (DeFuria et al., 2013). Recently, it was reported that B cells play an important role in postinfarct remodeling, where they infiltrate the ventricle and recruit monocytes (Zouggari et al., 2013). Therefore, precedents exist to support the contribution of B cells to myocardial remodeling. Interestingly, we saw fewer helper T cells in atria of patients with heart failure and AF compared with those with heart failure and in sinus rhythm. A reduction of helper T cells within the atrium was also reproduced in the dog model of sustained AF. It is likely that other T cell subtypes are increased in the fibrillating atrium, but we were not able to obtain adequate staining using several commercially available anti-CD3 antibodies to assess the total number of T cells.

However, the question remains as to whether adipocytes and B cell infiltration may be relevant players in atrial remodeling in patients with AF. We could not directly address this question in the present study, but interpretations are possible based on the existing literature. Sustained AF induces extreme metabolic stress upon the atrial myocardium, and B cells release significant amounts of macrophage migration inhibitor factor (Wymann et al., 1999), whereas adipocytes produce the adipokine D-dopachrome tautomerase (Iwata et al., 2012), which both inhibit AMP-dependent protein kinase activity through CD74 (Miller et al., 2008; Qi et al., 2014). It has recently been shown that adenosine monophosphate kinase is an important regulator of metabolic stress in the fibrillating dog atrium (Harada et al., 2015). Therefore, B cells and adipocytes may initially infiltrate the fibrillating atrium to modulate metabolic stress by releasing factors that inhibit adenosine monophosphate kinase, but later induce adverse structural remodeling that promotes sustained AF by releasing inflammatory cytokines.

Class I HDAC Inhibition and Cardiac Function. A major advantage offered by our dog model is the relative preservation of ventricular function during the entire duration of AF, without modifying atrioventricular node function. Therefore, by using echocardiography and chronically implanted probes, we could also assess the potential effects of class I HDAC inhibition on cardiac contractility and hemodynamics independent of AF. Although the effects of class I HDAC inhibition on AF and atrial remodeling are encouraging, we did not observe any improvement in cardiac function or chamber size, but we did see a slight reduction in the amount of MR during the 2-week treatment period. One reason explaining the lack of a significant improvement in cardiac function or chamber size may be related to the study design, since we left the dogs in sustained AF and never attempted to cardiovert them, either before or during the drug-treatment period.

Study limitations. The present investigation provides the proof of principle that class I HDAC inhibition can be considered as a possible new therapy for sustained AF. As mentioned in the *Materials and Methods*, the dose of CI-994 was chosen based on the hypothetical maximization of therapeutic effects while remaining within the limits of minimal toxicity. We did not observe harmful side effects in our dogs, and we did not expect any based on previous literature (Graziano et al., 1997). Subsequent studies will need to test lower doses and/or longer treatment periods, which might also lead to atrial size reduction, and, importantly, will need to determine whether the beneficial effects of class I HDAC inhibition on atrial remodeling and reduction in AF persist after interruption of the treatment. Finally, it will be interesting to test whether the combination of HDAC6 inhibitors, previously shown to prevent electrical remodeling in canine inducible AF (Zhang et al., 2014), and class I inhibitors can work synergistically in sustained AF, with even more pronounced beneficial effects than CI-994 alone.

Conclusions

Whereas we initially sought to determine if class I HDAC inhibition can reduce atrial remodeling and sustained AF, which our study results support, it is intriguing that we discovered previously unknown cellular effects related to atrial remodeling with sustained AF, such as intra-atrial B cell infiltration and increased adipocytes. Pan-HDAC inhibitors as well as CI-994 are already approved or being tested to cure various forms of cancer in humans (Pauer et al., 2004; Undevia et al., 2004; Monneret, 2005; Mann et al., 2007); therefore, the translational potential of our findings is encouraging. Given the failure of other pharmacological options for the treatment of sustained AF, the short-term inhibition of specific HDAC classes with agents administered at subtoxic doses might prove efficacious in stopping and perhaps reverting atrial remodeling with minimal or no damage of other organs.

Authorship Contributions

Participated in research design: Seki, LaCanna, Powers, Vrakas, Copper, Houser, Huang, Patel, Recchia.

Conducted experiments: Seki, LaCanna, Powers, Vrakas, Berretta, Chacko, Holten, Wang.

Contributed new reagents or analytic tools: Liu, Berretta, Jadiya, Wang, Arkles, Copper, Houser.

Performed data analysis: Seki, LaCanna, Powers, Vrakas, Liu, Chacko, Holten, Jadiya, Arkles, Huang.

Wrote or contributed to the writing of the manuscript: Seki, LaCanna, Powers, Vrakas, Patel, Recchia.

References

Abbaszadeh M, Khan ZH, Mehrani F, and Jahanmehr H (2012) Perioperative intravenous corticosteroids reduce incidence of atrial fibrillation following cardiac surgery: a randomized study. *Rev Bras Cir Cardiovasc* **27**:18–23.

Bradner JE, Mak R, Tanguturi SK, Mazitschek R, Haggarty SJ, Ross K, Chang CY, Bosco J, West N, and Morse E, et al. (2010) Chemical genetic strategy identifies histone deacetylase 1 (HDAC1) and HDAC2 as therapeutic targets in sickle cell disease. *Proc Natl Acad Sci USA* **107**:12617–12622.

Cappato R, Calkins H, Chen SA, Davies W, Iesaka Y, Kalman J, Kim YH, Klein G, Natale A, and Packer D, et al. (2010) Updated worldwide survey on the methods, efficacy, and safety of catheter ablation for human atrial fibrillation. *Circ Arrhythm Electrophysiol* **3**:32–38.

DeFuria J, Belkina AC, Jagannathan-Bogdan M, Snyder-Cappione J, Carr JD, Nersesova YR, Markham D, Strissel KJ, Watkins AA, and Zhu M, et al. (2013) B cells promote inflammation in obesity and type 2 diabetes through regulation of T-cell function and an inflammatory cytokine profile. *Proc Natl Acad Sci USA* **110**: 5133–5138.

El Khoury N, Mathieu S, and Fiset C (2014) Interleukin-1β reduces L-type Ca2+ current through protein kinase Cϵ activation in mouse heart. *J Biol Chem* **289**: 21896–21908.

Friedrichs K, Klinke A, and Baldus S (2011) Inflammatory pathways underlying atrial fibrillation. *Trends Mol Med* **17**:556–563.

Gaita F, Caponi D, Scaglione M, Montefusco A, Corleto A, Di Monte F, Coin D, Di Donna P, and Giustetto C (2008) Long-term clinical results of 2 different ablation strategies in patients with paroxysmal and persistent atrial fibrillation. *Circ Arrhythm Electrophysiol* **1**:269–275.

Grandy SA, Brouillette J, and Fiset C (2010) Reduction of ventricular sodium current in a mouse model of HIV. *J Cardiovasc Electrophysiol* **21**:916–922.

Grandy SA and Fiset C (2009) Ventricular K+ currents are reduced in mice with elevated levels of serum TNFalpha. *J Mol Cell Cardiol* **47**:238–246.

Graziano MJ, Pilcher GD, Walsh KM, Kasali OB, and Radulovic L (1997) Preclinical toxicity of a new oral anticancer drug, CI-994 (acetyldinaline), in rats and dogs. *Invest New Drugs* **15**:295–310.

Guo Y, Lip GY, and Apostolakis S (2012) Inflammation in atrial fibrillation. *J Am Coll Cardiol* **60**:2263–2270.

Haberland M, Carrer M, Mokalled MH, Montgomery RL, and Olson EN (2010) Redundant control of adipogenesis by histone deacetylases 1 and 2. *J Biol Chem* **285**: 14663–14670.

Harada M, Tadevosyan A, Qi X, Xiao J, Liu T, Voigt N, Karck M, Kamler M, Kodama I, and Murohara T, et al. (2015) Atrial Fibrillation Activates AMP-Dependent Protein Kinase and its Regulation of Cellular Calcium Handling: Potential Role in Metabolic Adaptation and Prevention of Progression. *J Am Coll Cardiol* **66**:47–58.

Ismat FA, Zhang M, Kook H, Huang B, Zhou R, Ferrari VA, Epstein JA, and Patel VV (2005) Homeobox protein Hop functions in the adult cardiac conduction system. *Circ Res* **96**:898–903.

Iwata T, Taniguchi H, Kuwajima M, Taniguchi T, Okuda Y, Sukeno A, Ishimoto K, Mizusawa N, and Yoshimoto K (2012) The action of D-dopachrome tautomerase as an adipokine in adipocyte lipid metabolism. *PLoS One* **7**:e33402.

Li D, Shinagawa K, Pang L, Leung TK, Cardin S, Wang Z, and Nattel S (2001) Effects of angiotensin-converting enzyme inhibition on the development of the atrial fibrillation substrate in dogs with ventricular tachypacing-induced congestive heart failure. *Circulation* **104**:2608–2614.

Li J, Patel VV, Kostetskii I, Xiong Y, Chu AF, Jacobson JT, Yu C, Morley GE, Molkentin JD, and Radice GL (2005) Cardiac-specific loss of N-cadherin leads to alteration in connexins with conduction slowing and arrhythmogenesis. *Circ Res* **97**:474–481.

Lin YK, Chen YC, Chen JH, Chen SA, and Chen YJ (2012) Adipocytes modulate the electrophysiology of atrial myocytes: implications in obesity-induced atrial fibrillation. *Basic Res Cardiol* **107**:293.

Liu F, Levin MD, Petrenko NB, Lu MM, Wang T, Yuan LJ, Stout AL, Epstein JA, and Patel VV (2008) Histone-deacetylase inhibition reverses atrial arrhythmia inducibility and fibrosis in cardiac hypertrophy independent of angiotensin. *J Mol Cell Cardiol* **45**:715–723.

Liu F, Lu MM, Patel NN, Schillinger KJ, Wang T, and Patel VV (2015) GATA-Binding Factor 6 Contributes to Atrioventricular Node Development and Function. *Circ Cardiovasc Genet* **8**:284–293.

Liu ZJ, Zhuge Y, and Velazquez OC (2009) Trafficking and differentiation of mesenchymal stem cells. *J Cell Biochem* **106**:984–991.

Liuba I, Ahlmroth H, Jonasson L, Englund A, Jönsson A, Säfström K, and Walfridsson H (2008) Source of inflammatory markers in patients with atrial fibrillation. *Europace* **10**:848–853.

Lkhagva B, Chang SL, Chen YC, Kao YH, Lin YK, Chiu CT, Chen SA, and Chen YJ (2014) Histone deacetylase inhibition reduces pulmonary vein arrhythmogenesis through calcium regulation. *Int J Cardiol* **177**:982–989.

Mann BS, Johnson JR, Cohen MH, Justice R, and Pazdur R (2007) FDA approval summary: vorinostat for treatment of advanced primary cutaneous T-cell lymphoma. *Oncologist* **12**:1247–1252.

Marrouche NF, Wilber D, Hindricks G, Jais P, Akoum N, Marchlinski F, Kholmovski E, Burgon N, Hu N, and Mont L, et al. (2014) Association of atrial tissue fibrosis identified by delayed enhancement MRI and atrial fibrillation catheter ablation: the DECAAF study. *JAMA* **311**:498–506.

Miller EJ, Li J, Leng L, McDonald C, Atsumi T, Bucala R, and Young LH (2008) Macrophage migration inhibitory factor stimulates AMP-activated protein kinase in the ischaemic heart. *Nature* **451**:578–582.

Mitacchione G, Powers JC, Grifoni G, Woitek F, Lam A, Ly L, Settanni F, Makarewich CA, McCormick R, and Trovato L, et al. (2014) The gut hormone ghrelin partially reverses energy substrate metabolic alterations in the failing heart. *Circ Heart Fail* **7**:643–651.

Monneret C (2005) Histone deacetylase inhibitors. *Eur J Med Chem* **40**:1–13.

Murin J, Naditch-Brûlé L, Brette S, Chiang CE, O'Neill J, and Steg PG (2014) Clinical characteristics, management, and control of permanent vs. nonpermanent atrial fibrillation: insights from the RealiseAF survey. *PLoS One* **9**:e86443.

Naccarelli GV, Varker H, Lin J, and Schulman KL (2009) Increasing prevalence of atrial fibrillation and flutter in the United States. *Am J Cardiol* **104**:1534–1539.

Özcan KS, Güngör B, Altay S, Osmonov D, Ekmekçi A, Özpamuk F, Kemaloğlu T, Yıldırım A, Tayyareci G, and Erdinler İ (2014) Increased level of resistin predicts development of atrial fibrillation. *J Cardiol* **63**:308–312.

Pauer LR, Olivares J, Cunningham C, Williams A, Grove W, Kraker A, Olson S, and Nemunaitis J (2004) Phase I study of oral CI-994 in combination with carboplatin and paclitaxel in the treatment of patients with advanced solid tumors. *Cancer Invest* **22**:886–896.

Qi D, Atsina K, Qu L, Hu X, Wu X, Xu B, Piecychna M, Leng L, Fingerle-Rowson G, and Zhang J, et al. (2014) The vestigial enzyme D-dopachrome tautomerase protects the heart against ischemic injury. *J Clin Invest* **124**:3540–3550.

Riley G, Syeda F, Kirchhof P, and Fabritz L (2012) An introduction to murine models of atrial fibrillation. *Front Physiol* **3**:296.

Shimano M, Shibata R, Tsuji Y, Kamiya H, Uchikawa T, Harata S, Muto M, Ouchi N, Inden Y, and Murohara T (2008) Circulating adiponectin levels in patients with atrial fibrillation. *Circ J* **72**:1120–1124.

Siwik DA, Chang DL, and Colucci WS (2000) Interleukin-1beta and tumor necrosis factor-alpha decrease collagen synthesis and increase matrix metalloproteinase activity in cardiac fibroblasts in vitro. *Circ Res* **86**:1259–1265.

Summers AR, Fischer MA, Stengel KR, Zhao Y, Kaiser JF, Wells CE, Hunt A, Bhaskara S, Luzwick JW, and Sampathi S, et al. (2013) HDAC3 is essential for DNA replication in hematopoietic progenitor cells. *J Clin Invest* **123**: 3112–3123.

Undevia SD, Kindler HL, Janisch L, Olson SC, Schilsky RL, Vogelzang NJ, Kimmel KA, Macek TA, and Ratain MJ (2004) A phase I study of the oral combination of CI-994, a putative histone deacetylase inhibitor, and capecitabine. *Ann Oncol* **15**: 1705–1711.

Venteclef N, Guglielmi V, Balse E, Gaborit B, Cotillard A, Atassi F, Amour J, Leprince P, Dutour A, and Clément K, et al. (2015) Human epicardial adipose tissue induces fibrosis of the atrial myocardium through the secretion of adipofibrokines. *Eur Heart J* **36**:795–805a.

Vieira-Potter VJ (2014) Inflammation and macrophage modulation in adipose tissues. *Cell Microbiol* **16**:1484–1492.

Woitek F, Zentilin L, Hoffman NE, Powers JC, Ottiger I, Parikh S, Kulczycki AM, Hurst M, Ring N, and Wang T, et al. (2015) Intracoronary Cytoprotective Gene Therapy: A Study of VEGF-B167 in a Pre-Clinical Animal Model of Dilated Cardiomyopathy. *J Am Coll Cardiol* **66**:139–153.

Wymann D, Blüggel M, Kalbacher H, Blesken T, Akdis CA, Meyer HE, and Blaser K (1999) Human B cells secrete migration inhibition factor (MIF) and present a naturally processed MIF peptide on HLA-DRB1*0405 by a FXXL motif. *Immunology* **96**:1–9.

Yamaguchi T, Cubizolles F, Zhang Y, Reichert N, Kohler H, Seiser C, and Matthias P (2010) Histone deacetylases 1 and 2 act in concert to promote the G1-to-S progression. *Genes Dev* **24**:455–469.

Yamashita T, Sekiguchi A, Iwasaki YK, Date T, Sagara K, Tanabe H, Suma H, Sawada H, and Aizawa T (2010) Recruitment of immune cells across atrial endocardium in human atrial fibrillation. *Circ J* **74**:262–270.

Yu T, Zhu W, Gu B, Li S, Wang F, Liu M, Wei M, and Li J (2012) Simvastatin attenuates sympathetic hyperinnervation to prevent atrial fibrillation during the postmyocardial infarction remodeling process. *J Appl Physiol (1985)* **113**: 1937–1944.

Yuan L, Wang T, Liu F, Cohen ED, and Patel VV (2010) An evaluation of transmitral and pulmonary venous Doppler indices for assessing murine left ventricular diastolic function. *J Am Soc Echocardiogr* **23**:887–897.

Zhang D, Wu CT, Qi X, Meijering RA, Hoogstra-Berends F, Tadevosyan A, Cubukcuoglu Deniz G, Durdu S, Akar AR, and Sibon OC, et al. (2014) Activation of histone deacetylase-6 induces contractile dysfunction through derailment of α-tubulin proteostasis in experimental and human atrial fibrillation. *Circulation* **129**:346–358.

Zoni-Berisso M, Lercari F, Carazza T, and Domenicucci S (2014) Epidemiology of atrial fibrillation: European perspective. *Clin Epidemiol* **6**:213–220.

Zouggari Y, Ait-Oufella H, Bonnin P, Simon T, Sage AP, Guérin C, Vilar J, Caligiuri G, Tsiantoulas D, and Laurans L, et al. (2013) B lymphocytes trigger monocyte mobilization and impair heart function after acute myocardial infarction. *Nat Med* **19**:1273–1280.

Address correspondence to: Dr. Fabio A. Recchia, Lewis Katz School of Medicine, Medical Education and Research Building 1054, 3500 North Broad Street, Philadelphia, PA 19140. E-mail: fabio.recchia@temple.edu or Dr. Vickas Patel, Lewis Katz School of Medicine, MERB 1058, 3500 North Broad Street, Philadelphia, PA 19140. E-mail: vickas.patel@temple.edu